

# DESIGN OF THE MAGNETIC SHIELD FOR TRASCO LOW BETA ELLIPTICAL CAVITIES

P. Pierini, S. Barbanotti, L. Monaco, N. Panzeri, INFN Milano - LASA

## Abstract

The TRASCO elliptical cavities ( $\beta=0.47$ ) for intermediate velocity protons will be tested in horizontal test modules, equipped with a coaxial cold tuner of the blade type. A magnetic shield which is internal to the helium vessel has been designed, using CRYOPERM 10 material. The magnetic shield is capable to meet the performance goals of the 700 MHz cavities and simplifies the mechanical interface to the cavity/tuner assembly. The present paper illustrates the technical design of such a shielding system.

## THE TRASCO CAVITY AND COAXIAL TUNING SYSTEM

As part of the TRASCO program in the past years two multicell superconducting cavities of the elliptical type have been designed, build and extensively tested for the design of an ADS system based on a superconducting linac [1, 2]. Both cavities (shown in Figure 1) outreached the nominal specifications (8.5 MV/m of accelerating field at a Q value larger than  $5 \cdot 10^9$ ) with a considerable operational margin. The cavities have been tested at TJNAF and Saclay [3] and reached peak electric and magnetic fields of 61 MV/m and 100 mT, respectively, with performances similar to the standard TTF cavities production. In both tests the cavity performance was limited by field emission at high fields, and considering the peak electric field on the surface, the performance limits were compatible with a BCP treated TESLA cavity shape in the 25-30 MV/m range.

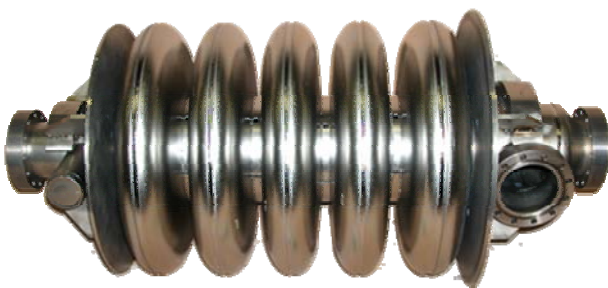


Figure 1: The bare TRASCO cavity.

A “blade” tuner, derived from the one successfully tested in the TTF and proposed for the ILC linac [4], has been developed and fabricated for the two cavities [5] (Figure 2). This coaxial device will allow both a slow and a fast, piezo-assisted, tuning action for the dynamic compensation of the Lorentz force detuning in pulsed operation. The two cavities, completely equipped with tuning system and under operating conditions, will be tested in the EUROTRANS [6] and CARE/HIPPI programs [7] of the 6<sup>th</sup> FP of the EC in the near future.



Figure 2: The He-tank and tuner assembly for the TRASCO cavities.

One cavity will be tested for high power pulsed operation for Lorentz Force Detuning compensation experiments in CRYHOLAB and the second will be tested in high power CW operation and microphonics control in a prototypical cryomodule for ADS activities.

Table 1 resumes the cavity design parameters.

Table 1: Main 5 cell Cavity Parameters

Parameter	Value
Design Frequency	704.4 MHz
Geometrical $\beta$	0.47
Iris radius	40 mm
Cell to cell coupling	1.34 %
R/Q	180 Ohm
G	160 Ohm
$E_{peak}/E_{acc}$	3.57
$B_{peak}/E_{acc}$	5.88 mT/(MV/m)
Stiffening ring radial position	70 mm
Cavity longitudinal stiffness ( $K_{cav}$ )	1.248 kN/mm
Frequency sensitivity (longitudinal)	-353.4 kHz/mm
Vacuum freq. coeff. (constrained)	84.7 Hz/mbar
Vacuum reaction force at boundary	3.7 N/mbar
Lorentz coefficient (constrained)	-3.7 Hz/(MV/m) <sup>2</sup>
Lorentz reaction force at boundary	0.177 N/(MV/m) <sup>2</sup>

In the various vertical tests, the static Lorentz force detuning coefficient derived from the frequency data ranges from -20 to -47 Hz/(MV/m)<sup>2</sup>. The spread in the resulting  $K_L$  value, although greater than the value listed in

Table 1 is due to the limited stiffness of the support frames used in the experimental setups, intended to constrain the cavity length during testing. A model was developed to understand the data by taking into account the finite stiffness of the TJNAF and Saclay supports [8].

The results obtained by this study were used to set the overall longitudinal stiffness of the tuner-He tank system, in order to be able to operate these low beta elliptical structures stable conditions either from LFD effects and capabilities of microphonics control.

In both the experimental conditions foreseen for the cavities, the earth magnetic field needs to be shielded efficiently from the niobium cavity surfaces in order not to increase the surface resistivity due to magnetic field trapping and limit the cavity performances.

### THE INNER MAGNETIC SHIELD

The coaxial tuner is located outside the cavity He tank, thus a solution based on an external shield enclosing the cavity-tuner assembly would result in a large size for the shell enclosure needed for shielding, imposing relevant clearance constraints and limiting access to the tuner mechanical components. For these reasons, we are investigating the possibility of using a magnetic shield located internally to the cavity He tank, in order to limit the amount of expensive CRYOPERM material and provide a simple and effective design.

#### Required shielding factor

The wall losses on the cavity surfaces are determined by the surface resistance, which has contributions arising from several physical phenomena:

$$R_{surf} = R_{BCS}(v, T) + R_{res} + R_{mag}(H_{ext}) \quad (1)$$

The first fundamental term comes ( $R_{BCS}$ ) from the BCS theory and depends on the temperature and to the square on the RF frequency [9]. At 704.4 MHz, 2 K the BCS term accounts for a contribution of 3.2 nΩ.

The second term, the residual resistance, is related to the technology of the cavity fabrication and treatment processes and can arise from various sources (foreign material inclusions during fabrication, residues of chemical etching, condensed gases, ...).

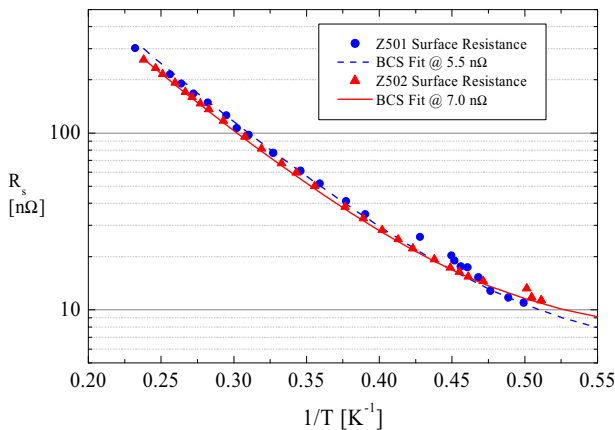


Figure 3:  $R_s$  values from RF measurements.

Figure 3 shows the comparison of the surface resistance estimations derived from the vertical RF tests with the fit to the BCS model, which gives an estimation of the residual resistance term in the range of a few (5-7) nΩ [3].

The last term in equation 1 is due to the pinning and trapping of DC magnetic flux (typically the earth magnetic field) in the superconductor. For high RRR niobium this contribution can be estimated as

$$R_{mag} = 3 [n\Omega] \langle H_{ext} [\mu T] \rangle \sqrt{v [GHz]} \quad (2)$$

where  $\langle H_{ext} \rangle$  is the average magnetic field flux seen by the cavity surface.

Finally, the surface resistance and the quality factor of the resonator are related through the cavity geometrical factor  $G = R_{surf} Q$ , which for the TRASCO cavity has the value of 160 Ω. Figure 4 shows the expected Q as a function of the average surface field on the cavity walls (for the two values of the residual resistance determined from the RF tests). Values of 2-3 μT are sufficient to achieve a goal Q at the 10<sup>10</sup> level.

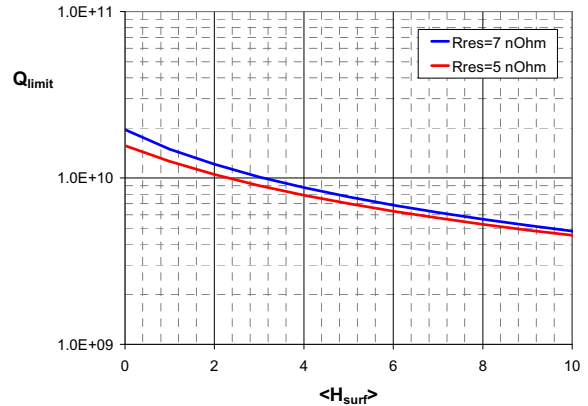


Figure 4: Cavity expected Q as a function of the average magnetic field on the surface (units of μT).

#### Shield performances

The performance of the 1 mm thick Cryoperm shield against a 30 μT field oriented along the cavity axis has been analyzed with an axially symmetric model. Figure 5 shows the computed surface fields.

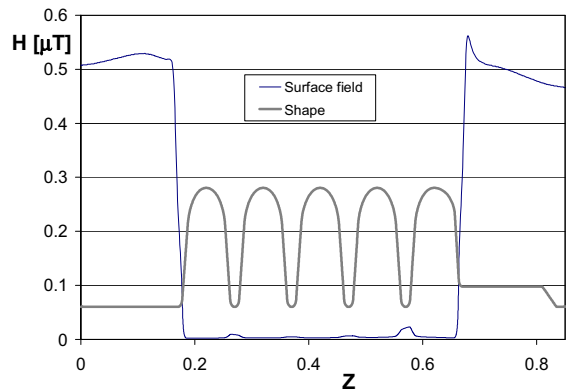


Figure 5: Field levels along the cavity surface (the cavity profile is shown for clarity), for a 30 μT axial field

Even if the internal shield is ineffective in the beam tube regions, where the external ambient field reaches the niobium surfaces, the average field computed on the overall cavity surface exposed to the RF field is kept below the desired level of 3  $\mu$ T.

*Shield design*

The shield is composed by 1 mm thickness CRYOPERM 10 sheets and is located across the cavity, internal to the He tank. The shield is supported at the cavity tubes by means of small G10 blocks, that separate the high permeability metal from the niobium surfaces at the tube and avoid contact to the end irises due to the differential shrinkage of materials. The shield is mainly composed of three parts: two split end dishes at the cavity ends, and a tube. The tube allows the longitudinal adjustment to the final cavity length and can be laterally inserted from one side, where the smaller diameter He tank support dish is located.

Figure 6 shows the lateral view of the cavity, indicating the main geometrical constraints for the shield design. To the left side the smaller diameter end dish is clearly visible. We note here that the cavity length (i.e. the distance between the end dishes) is the nominal fabrication distance and a 10-15 mm regulation is needed to account for the cavity length adjustment that was needed to bring each cavity to the correct nominal frequency and with a good field flatness.

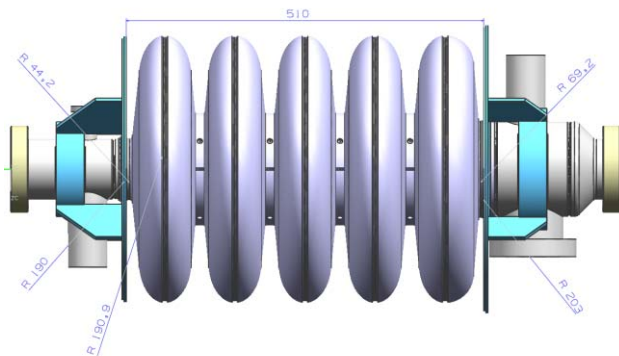


Figure 6: Lateral view of the TRASCO cavity, indicating the main geometrical constraints for the shield design.

Figure 7 shows the internal magnetic shielding assembled around the cavity, before the final weld of the He vessel to the end dishes. The end parts of the shield are shaped in order to keep them at a distance from the region where the weld to the He tank need to be performed, in order to limit the possibilities of heating them during the weld operations and deteriorate the high permittivity of the material.

The slotted ends at the connections from the end shields to the tube allow the longitudinal adjustment to the final cavity length and to provide a good contact between the different shield parts in order to avoid field leaking. Moreover, small (3 mm diameter) holes are foreseen on the shield tube to allow He gas flow during cooldown.



Figure 7: The shield around the cavity.

The shield tube slides from the left cavity side and is superimposed on the right end shield end pieces (which has an outer diameter matching that of the inner shield tube, whereas the left shield end has an inner diameter matching that of the outer shield tube). The longitudinal sectioning and adjustment capabilities of the shield is better illustrated by the following figure.

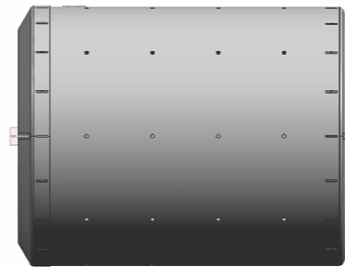


Figure 8: Longitudinal view of the shield assembly, showing the length adjustment capabilities through the slotted/threaded pairs on the segments, which allow for a good magnetic contact between the shield portions.

The following figure shows the sequence of the assembly procedure of the main shield components.

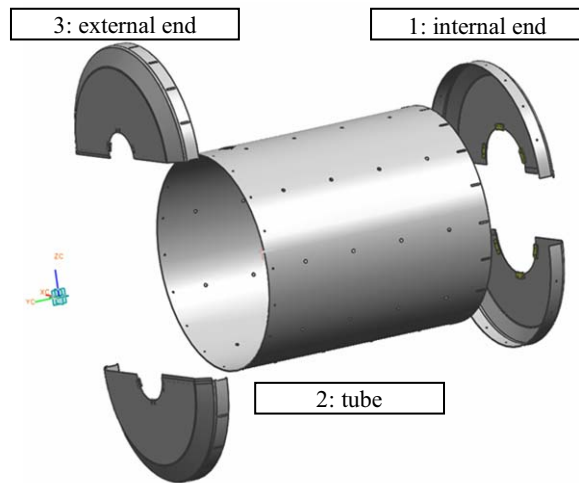


Figure 9: Assembly procedure for the shield portions.

First, the smaller diameter end shield pieces (“internal” end) are assembled at the coupler end of the cavity (larger

beam tube). The figure shows also the G10 connections parts that prevent the shield from touching the cavity walls. The end dish have threaded holes to provide contact with the other shield segments (or, as suggested by the vendor, small threaded plates, not shown here in the models, are spot welded to the shield to ensure the proper magnetic contact).

Then the shield tube is slid from the left side of the cavity (pickup port side, where the Ti dish for the He tank connection has a smaller diameter and the shield is fastened to the right end portions).

Finally, the two halves of the external end at the left cavity side are connected externally to the internal tube and fastened to it, using the same mechanism than before.

At this point the He tank can be inserted (again, from the left side of the cavity and welded to the support dishes. After the He tank integration a small Cryoperm pipe can then be inserted and fastened to the large hole in the inner tube (for the He gas exhaust flow), to minimize the field penetration.

Figure 10 shows a section of the final assembly, after integration of the system in the He tank.

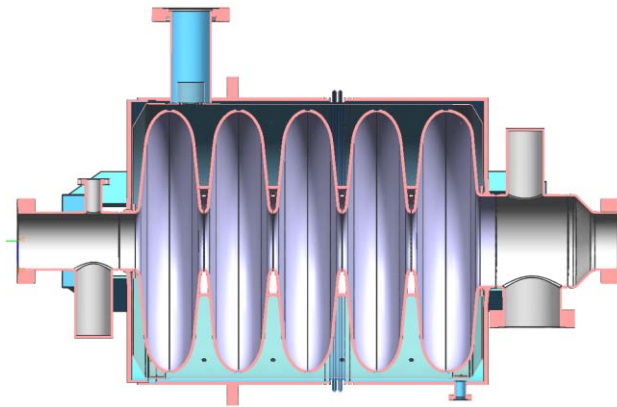


Figure 10: A section view of the complete assembly of the inner magnetic shield inside the He tank.

Finally, in order to ensure a good contact and protection against penetration of the longitudinal field across the end shield segments, a spot-welded lip connecting the two end halves is used to guarantee good contact between the high  $\mu$  material, as shown in Figure 11.

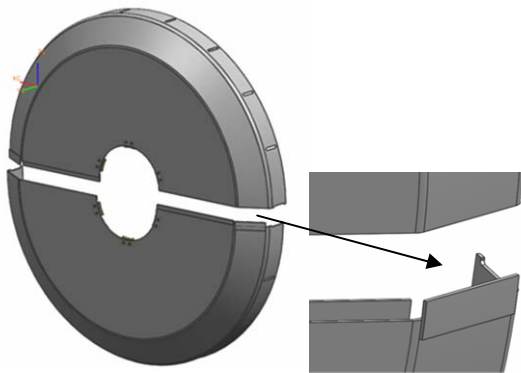


Figure 11: Detail of the end shield segments, with the spot welded lips to ensure minimal axial field penetration.

The final configuration of the He tank is then shown in Figure 12, with an indication of the region where the final regulation weld on the two tank halves is performed.

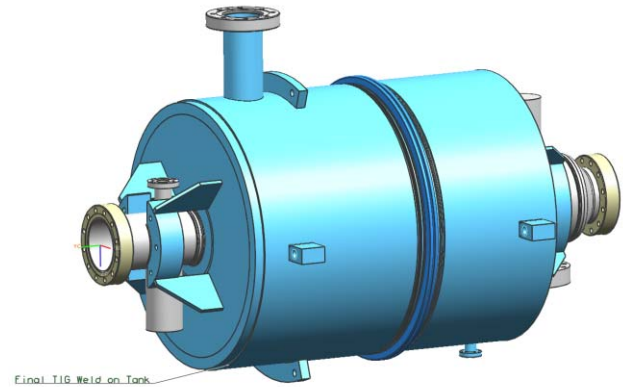


Figure 12: The final configuration of the He tank.

## CONCLUSIONS

The moderate RF frequency of the TRASCO cavities and the performances required for their operation by the linac design ( $E_{acc}=8.5$  MV/m at  $Q = 5 \cdot 10^9$ ) allowed to investigate the possibility of a simple magnetic shield solution which is internal to the cavity Helium tank. This solution, although less efficient from the shielding point of view compared to an external enclosure of the cavity which covers the beam tubes with continuity in the shielding material, is attractive for its simplicity and cost. Two shields are currently being procured and will be used for the horizontal tests of the cavities under the HIPPI and EUROTRANS programs.

## ACKNOWLEDGEMENTS

This work is partially supported by the EURATOM 6<sup>th</sup> Framework Program (FP6) of the EC under contract FI6KW-CT-2004-516520 (EUROTRANS) and by the European Community-Research Infrastructure Activity under the FP6 "Structuring the European Research Area" program (CARE, contract number RII3-CT-2003-506395).

## REFERENCES

- [1] D. Barni, A. Bosotti, G. Ciovati, C. Pagani, P. Pierini, "SC Cavity Design for the 700 MHz TRASCO Linac", in Proceedings of EPAC 2000, Vienna, Austria.
- [2] J.L. Biarrotte, H. Safa, J.P. Charrier, S. Jaidane, H. Gassot, T. Junquera, J. Lesrel, G. Ciovati, P. Pierini, D. Barni, C. Pagani, "704 MHz Superconducting Cavities for a High Intensity Proton Accelerator", in Proceedings of the 1999 RF Superconductivity Workshop, Santa Fe, USA.
- [3] A. Bosotti et al., "RF Tests Of The Beta=0.5 Five Cell TRASCO Cavities", Proceedings of EPAC 2004, Lucerne, Switzerland, p. 1024.
- [4] See C. Pagani et al., "Piezo-Assisted Blade Tuner: Cold Test Results", these Proceedings and references therein for the blade tuner design.

- [5] P. Pierini et al., "Report on Tuner Design", CARE-Note-2006-003-HIPPI, available from <http://www-dapnia.cea.fr/Documentation/Care/index.php>.
- [6] S. Barbanotti et al., "The prototype cryomodule for the EUROTRANS program", these Proceedings, contribution WEP83.
- [7] See <http://mgt-hippi.web.cern.ch/mgt-hippi/> for a description of the HIPPI program.
- [8] A. Bosotti et al., "Characterization of an Elliptical Low Beta Multicell Structure for Pulsed Operation", in Proceedings of the 12<sup>th</sup> SRF Workshop, Cornell, USA.
- [9] H. Padamsee, J. Knobloch, T. Hays, "RF Superconductivity for Accelerators", Wiley Series in Beam Physics and Accelerator Technology, John Wiley and Sons, New York, 1998.